Dynamic Nuclear Polarization in Pulsed ENDOR Experiments

Vladimir Kouskov,* David J. Sloop,* Shang-Bin Liu,† and Tien-Sung Lin*,1

*Department of Chemistry, Washington University, St. Louis, Missouri 63130; and †Institute of Atomic and Molecular Sciences,
Academia Sinica, P.O. Box 23-166, Taipei, Taiwan 10764

Properly prepared pulse sequences of microwave and radio frequency have been employed to investigate the effect of polarization transfer from the polarized photo excited triplet state of pentacene in *p*-terphenyl crystals to the surrounding protons in pulsed ENDOR experiments. The ENDOR signal, measured as the change of electron spin echo (ESE) amplitude, is affected by the mode of RF pulses. When $B_0 \| x$ (the long molecular axis), the ESE amplitude of the high-field transition of the triplet state changes from the maximum positive to zero with a π RF pulse, and to the maximum negative with a 2π pulse, while that of the low-field transition changes from nearly zero to the maximum negative as the RF pulse width increases. The effect is attributed to the strong electron spin polarization produced in the creation of the photoexcited triplet state and the subsequent efficient electron–nuclear polarization transfer process. © 1999 Academic Press

Key Words: ENDOR; DNP; pulsed EPR; triplet state; organic solids.

INTRODUCTION

The conventional ENDOR signal is observed through the desaturation of an EPR transition by inducing nuclear transitions. The effect, driven by a complicated balance of relaxation processes, weakly affects signal amplitude that limits the application of the cw technique (*1*). The anticipated ENDOR amplitude is about 1% of the EPR signal intensity. The ENDOR signal is expected to be even weaker in the photoexcited triplet state of organic systems, because of low triplet concentration due to either low solubility or short lifetime. Thus, most of the cw ENDOR experiments of organic triplet states have been performed in single crystals and at liquid helium temperatures.

However, pulsed ENDOR techniques have been developed to overcome some of the drawbacks of the cw technique (*2–5*). The pulsed experiments often employ three microwave pulses, and a radiofrequency pulse which is applied between the second and the third microwave pulses (*3*). At nuclear resonance, the applied RF pulse flips the nuclear spins, resulting in a change of the local field at the electron site. During the refocusing period after the third microwave pulse, the electron

spins that have had their precessional frequencies changed come together in different directions in the *xy* plane and differ from the other electron spins. The process results in a loss of phase coherence and a reduction of the electron spin echo (ESE) amplitude.

Two new pulsed ENDOR techniques have also been reported by Mehring and his co-workers: the spinor-ENDOR effect (*6*) and the high resolution coherence transfer ENDOR method (*7*). The spinor-ENDOR technique utilizes the 4π rotational symmetry of a proton coupled to an electron to achieve a 200% ENDOR effect. The coherence transfer ENDOR technique provides a method to obtain high-resolution ENDOR spectra. Initially, well-defined pulses are applied simultaneously to EPR ($P_{0S} = \pi$) and NMR ($P_{0I} = \pi/2$) transitions. The nuclear spin manifold is then subjected to a second RF pulse, $P_{1I} = \pi/2$, at a time *t* after the initial preparation pulse. The coherence of prepared nuclear sublevels can be transferred back to the EPR transition. Two microwave pulses ($P_{1S} = \pi/2$, $P_{2S} = \pi$) are applied after P_{1I} to create an ESE whose amplitude is a measure of the sublevel magnetization. The time *t* is incremented in steps and allows the completed FID to be mapped out. After FFT of the FID, a highly resolved ENDOR spectrum is obtained.

Previously we reported a pulsed ENDOR study on the photoexcited triplet state of pentacene in *p*-terphenyl crystals (PHTH) at room temperature (*8, 9*). Recently we have implemented many improvements in our pulsed ENDOR spectrometer, such as the addition of a frequency synthesizer, multiple NMR pulses, and better detection arrangements. Here we employ an ENDOR scheme, similar to Davies' sequence (*4*), but with a variable RF pulse duration in our experiments. The objectives of our study are to study the variation of longitudinal magnetization of electron spin as a function of RF pulse width, and to determine the optimal conditions to achieve maximum ENDOR enhancement. We also attempt to examine the effect of dynamic nuclear polarization of the photoexcited triplet state of the PHTH system at room temperature.

EXPERIMENTAL

A pulsed X-band EPR spectrometer was employed in the study. A special ENDOR cavity with multiple-turn NMR coils

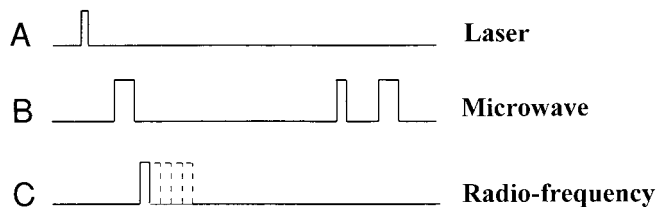1 To whom correspondence should be addressed. Fax: (314) 935-4481; E-mail: lin@wuchem.wustl.edu.

FIG. 1. The pulse sequences employed in the pulsed ENDOR experiments: (A) laser pulse, (B) microwave pulses (π–$\pi/2$–π), and (C) radiofrequency pulses.

wound around the sample was used in the measurement, which is similar to the setup used in the previous pulsed transient nutation experiments (*10*).

The pulse sequence used in our pulsed ENDOR experiments is the following (see Fig. 1): [(laser pulse)–t_1–($\pi\mu$wave pulse)–t_2–(RF pulse)–t_3–($\pi/2$ μwave pulse)–τ–(π μwave pulse)–τ–echo], where the laser pulse is used to excite the molecule to the metastable triplet state. The timing sequence of boxcar gate pulses and lock-in amplifier to reduce the background noise and to improve baseline correction are similar to those of our previous pulsed ENDOR experiments (*9*).

In our previous pulsed EPR studies of the photoexcited triplet state of the pentacene molecule (*11*), we observed that the initial triplet population of PHTH upon laser excitation is predominantly in the $|0\rangle$ substate ($m_S = 0$) for $B_0\|x$ (the molecular long axis). The application of the first π microwave pulse is therefore to create the longitudinal electron magnetization, $\langle S_Z\rangle$, by inverting the population of the $|0\rangle$ with the $|+1\rangle$ sublevel for the high-field (HF) transition (absorptive signal), and the $|0\rangle$ with the $|-1\rangle$ for the low-field (LF) transition (emissive signal). We further apply an RF pulse with variable duration (0 to 15 μs) at a fixed ENDOR frequency immediately after the microwave pulse, and at about 0.5 μs after the laser pulse. Since the electron T_1 is ~20 μs, we are able to monitor the time evolution of electron magnetization after the first π microwave pulse upon the application of the RF pulse to induce nuclear transitions. The $\langle S_Z\rangle$ as a function of time during the RF pulse is monitored by the last two microwave pulses, the conventional two-pulse echo sequence.

RESULTS AND DISCUSSION

The echo amplitude as a function of RF pulse width for the HF and LF transitions of the photoexcited triplet state of the PHTH system for $B_0\|x$ at the proton frequencies of 15 and 13 MHz, respectively, is shown in Fig. 2. The echo amplitude of the HF transition changes from the maximum positive (I = 4.2 ± 0.1 arbitrary unit) to zero at a duration time equivalent to the π pulse (3 μs) of the RF field, and to the maximum negative echo at the 2π pulse (I = −2.7 ± 0.1). Here the change of echo amplitude follows roughly a sinusoidal period for the first several microseconds. Physically, the microwave π pulse on the HF line causes a sudden change in the magnitude

of the effective B_Z at the proton sites. However, this *new* field is tilted only slightly from the original B_0, judging from the weak ESE envelope modulation (ESEEM) observed in our previous studies (*11*), i.e., the protons are weakly coupled to the electron spin in the $|+1\rangle$ sublevel. The combination of the π EPR pulse and the following RF pulse (with variable duration) should result in an oscillating B_Z term at the electron site. Thus, in principle, we should observe Rabi oscillation as a function of RF pulse duration. However, the observed nonsinusoidal behavior after 8 μs (one-half cycle period) may arise from the dephasing of the electron spin magnetization due to cross-polarization processes at the time of detection.

On the other hand, the echo amplitude of the LF transition as a function of the RF pulse duration shows no oscillatory behavior. The echo amplitude of the LF resonance changes from nearly zero (I = −0.4 ± 0.1) at a duration less than 1 μs of the RF pulse to the maximum negative (I = −2.0 ± 0.1) at 11 μs as the RF pulse width increases. Here, upon the application of a long RF pulse, the ESE signal changes from almost null amplitude to a factor of *four* larger.

We observed the maximum changes of ESE amplitude (ENDOR enhancement) when the RF pulses were applied at the
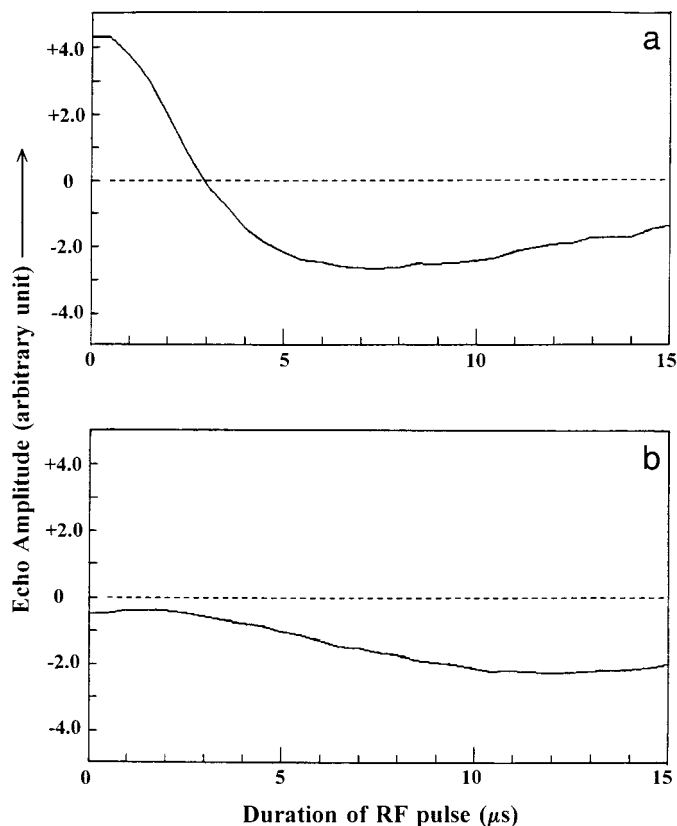

FIG. 2. The ENDOR intensity (echo amplitude) vs the RF pulse duration for the photoexcited triplet state of pentacene in *p*-terphenyl crystals, $B_0\|x$: (a) high-field (HF) transition at 3541 G, and (b) low-field (LF) transition at 2992 G. The dead time of the detection was ~0.5 μs. The frequencies of RF pulses were set at 15 and 13 MHz for the HF and LF transitions, respectively.

free proton frequencies: 13 MHz for the LF transition and 15 MHz for the HF transition. These frequencies correspond to the nuclear transitions in the $|0\rangle$ manifold where there is no first-order hyperfine interaction, i.e., proton Zeeman term only. We observed less ENDOR intensity when RF pulses were applied at other than the above free proton frequencies. We should point out that these free proton ENDOR signals are light sensitive; therefore, they belong to the protons in the photoexcited triplet state of the pentacene molecule, and not those of the host molecules.

The peculiar enhancement of ENDOR signals may be explained in terms of the effect of RF field on the phase coherence of spin packets. The EPR lines of solids are inhomogeneously broadened, consisting of many spin packets (hyperfine isochromats). In the LF transition, the first π EPR pulse causes long-term irreversible mixing of the nuclear and electron spin states. Since we observed little or no echo at a particular pulse interval of the two-pulse sequence in the LF transition, the spin packets in the inhomogeneous line may be shifted out-of-phase upon the application of the first microwave π pulse. The effect is attributed to the dominant non-secular hyperfine terms. The hyperfine terms may be expressed to the first order as follows,

$$\mathbf{H}_{\mathrm{hf}} = \sum_i S_z(A^i I_z^i + B^i I_x^i), \qquad [1]$$

where i refers to the ith proton. The A^i terms (secular terms) determine the spectral line position, and the B^i terms (nonsecular) induce mixing among hyperfine levels. In the LF transition, the hyperfine terms of some protons are dominated by nonsecular terms, i.e., $B^i > A^i$, which yield deep ESEEM (*11*). One may reexpress the nonsecular hyperfine terms up to the second order and keep the flip-flop terms in the effective Hamiltonian (*10, 12*):

$$\mathbf{H}_{\mathrm{eff}} \propto \sum_i (A_{+z}^i I_-^i \sigma_+ + A_{-z}^i I_+^i \sigma_-), \qquad [2]$$

where $A_{\pm z}^i = A_{xz}^i \pm iA_{yz}^i$, $I_\pm^i = I_x^i \pm iI_y^i$, and $\sigma_\pm = \sigma_x \pm i\sigma_y$ (the Pauli matrices for the fictitious two-level of the electron spin).

The large nonsecular hyperfine terms can give rise to the observed irreversible damping of the ESE signals in the LF transition. Here the effective field at the positions of the electron spin and nuclear spins are *not parallel* to each other in the $|-1\rangle$ substate. Thus, an electron spin flip upon the application of a microwave pulse will cause a large change in the direction of the effective field. This off-diagonal coherence is clearly present as evidenced from the recovery of electron spin polarization by applying an RF pulse after the EPR π pulse. In other words, the application of properly prepared NMR pulses can shuffle the hyperfine isochromats and force the spin packets to shift back in-phase to give rise to an increase in the echo amplitude.

Moreover, the nonoscillatory behavior observed in the LF transition may arise from the effective polarization transfer of the polarized triplet electron spin to the surrounding protons under the influence of the RF pulse. A combination of microwave and RF pulse sequences can bring both the electron spin and nuclear spins into resonance and cause an effective polarization transfer to the surrounding protons at the free proton frequencies. Here the Rabi frequency of the electron spin system (rotating frame in the preparation π pulse) was made to *approximately* match the Lamor frequency of the nuclear system (laboratory frame) to fulfill the Hartmann–Hahn condition for an effective polarization transfer. Previously, we have also observed similar effects in the pulsed transient nutation experiments where the spectral diffusion and polarization transfer processes in the LF transition are one order of magnitude greater than those of the HF transition (*10*). The effective polarization transfer in the LF transition is attributed to the substantial contribution from the nonsecular hyperfine terms. Contrarily, when the RF is applied at other than the free proton frequencies, the electron–nuclear polarization transfer is less effective and gives rise to less ENDOR intensity.

On the other hand, the HF transition is dominated by the secular hyperfine components, $A^i > B^i$. Thus, the effective fields at the positions of the electron spin and nuclear spins are *nearly parallel* to each other in the $|+1\rangle$ substate. The applied microwave and RF pulses are effective rotation operators. Both can shift the spin packets away from each other, which can lead to a decrease in echo intensity after the application of RF pulses. The rotation operators presumably induce enough irreversible perturbation to cause the effect to die out after the first half-cycle of oscillation.

Finally, we should emphasize that the ENDOR effects of an $S = 1$ system with strong spin polarization and peculiar partitioning of electron–nuclear spin manifold are very different from those of an $S = \frac{1}{2}$ system. In our case, the $|0\rangle$ state does not have a first-order hyperfine interaction. Thus, there is always a large *uncoupled* proton contribution to the observed ENDOR effect. The Davies ENDOR pulse sequence admixes $|0\rangle$ with $|+1\rangle$, or $|0\rangle$ with $|-1\rangle$ states. The flipping of proton spins during the RF pulse in the *collapsed, uncoupled line-shape* can therefore greatly affect the electron spin time evolution while reforming the echo even when the electron spin is later in the $|+1\rangle$ or $|-1\rangle$ state. This peculiar effect does not occur in the doublet states where both the upper and lower states have the first-order hyperfine interaction. A theoretical treatment, applying the spin rotation operators and time evolution operators and utilizing the density matrix formalism to simulate the observed ENDOR effect, is in progress.

In summary, we have demonstrated a peculiar effect in pulsed ENDOR experiments of the photoexcited triplet state of the pentacene molecule: the behaviors (degree of enhancement and oscillation) of the HF transition differ from those of the LF one. We further investigated the dynamic aspects of the electron–nuclear interaction: properly prepared microwave and RF pulses can bring both the electron spin and nuclear spins into

resonance to achieve an effective cross-polarization, and achieve the maximum ENDOR signal. Furthermore, the long duration of RF pulses in our ENDOR experiments may behave as transient nutation pulses, and possibly cause the observed irreversible signal decay. Thus, the observed pulsed ENDOR spectra may be taken as the responses of the transient nutation of nuclear spin systems onto the ESE amplitude.

ACKNOWLEDGMENTS

REFERENCES

1. L. Kevan and L. D. Kispert, "Electron Spin Double Resonance Spectroscopy," Wiley, New York (1976).

2. C. Gemperle and A. Schweiger, Pulsed electron–nuclear double resonance methodology, *Chem. Rev.* **91**, 1481–1505 (1991), and references therein.

3. W. B. Mims, Electron spin echo, in "Electron Paramagnetic Resonance" (S. Geschwind, Ed.), Chap. 4, Plenum Press, New York (1972).

4. E. R. Davies, A new pulse ENDOR technique, *Phys. Lett.* **47A**, 1–2 (1974).

5. W. A. J. A. van der Poel, D. J. Singel, J. Schmidt, and J. H. van der Waals, Pulsed ENDOR spectroscopy of the interior protons of free-base porphin in its lowest photoexcited triplet state in an *n*-octane single crystal, *Mol. Phys.* **49**, 1017–1028 (1983).

6. M. Mehring, P. Hoffer, A. Grupp, and H. Seidel, Spinor-ENDOR: 200% effect, *Phys. Lett.* **106A**, 146–150 (1984).

7. P. Hoffer, A. Grupp, and M. Mehring, High resolution coherence transfer ENDOR, *Phys. Rev.* **A33**, 3519–3622 (1986).

8. T.-S. Lin, J.-L. Ong, D. J. Sloop, and H.-L. Yu, Spin-echo ENDOR Studies of Organic Triplets at Room Temperature, in "Pulsed EPR: A New Field of Applications" (C. P. Keijzers, E. J. Rijerse, and J. Schmidt, Eds.), pp. 191–195, North Holland, Amsterdam (1989).

9. D. J. Sloop and T.-S. Lin, Spin-echo-ENDOR studies of the photoexcited triplet state of pentacene in *p*-terphenyl crystals at room temperature, *J. Magn. Reson.* **86**, 156–159 (1990).

10. V. Kouskov, D. J. Sloop, S.-B. Liu, and T.-S. Lin, Pulsed transient nutation experiments of the photo excited triplet state, *J. Magn. Reson. A* **117**, 9–15 (1995).

11. D. J. Sloop, H.-L. Yu, T.-S. Lin, and S. I. Weissman, Electron spin echoes of a photoexcited triplet: Pentacene in *p*-terphenyl crystals, *J. Chem. Phys.* **75**, 3746–3757 (1981).

12. D. J. van den Heuvel, A. Henstra, T.-S. Lin, J. Schmidt, and W. Th. Wenckebach, Transient oscillations in pulsed dynamic nuclear polarization, *Chem. Phys. Lett.* **188**, 194–199 (1992).